

Pulse Dispersion Properties of Fibers with Various Material Constituents

By L. G. COHEN, F. V. DIMARCELLO, J. W. FLEMING,
W. G. FRENCH, J. R. SIMPSON, and E. WEISZMANN

(Manuscript received November 11, 1977)

Intermodal dispersion properties are compared for high silica fibers with borosilicate (B_2O_3 - SiO_2) and germania borosilicate (GeO_2 - B_2O_3 - SiO_2) graded-index profiles. Pulse transmission measurements were systematically correlated with profile shapes so that new fibers could be fabricated with closer-to-optimal profile gradients at a wavelength of 907.5 nanometers. Germania borosilicate fibers with power law profile exponents ($\alpha \approx 2.03$) lowered intermodal dispersion 50 times from the result expected for comparable step-index fibers with $N.A. \approx 0.19$. By contrast, borosilicate fibers with $\alpha \approx 1.78$ caused a 100-fold pulse width reduction in fibers with $N.A. \approx 0.14$, corresponding to a $2\sigma = 0.13$ ns/km pulse-broadening rate.

I. INTRODUCTION

Dispersive refractive index differences between material constituents (GeO_2 , B_2O_3 , and SiO_2) for germania borosilicate core fibers cause modal group velocity differences to depend on the source wavelength (profile dispersion). Therefore, nonparabolic profile gradients are generally required to minimize pulse dispersion.

Previous time-domain transmission measurements^{1,2} were used to direct the fabrication of a nearly optimal borosilicate fiber. This paper compares more recent and extensive data for germania borosilicate fibers and borosilicate fibers at $\lambda = 907.5$ nm wavelength corresponding to a GaAs injection laser. We have also characterized small profile undulations about a nearly optimal power law shape which degrade intermodal dispersion characteristics. Another paper³ describes how profile dispersion influences fiber bandwidth properties at other wavelengths.

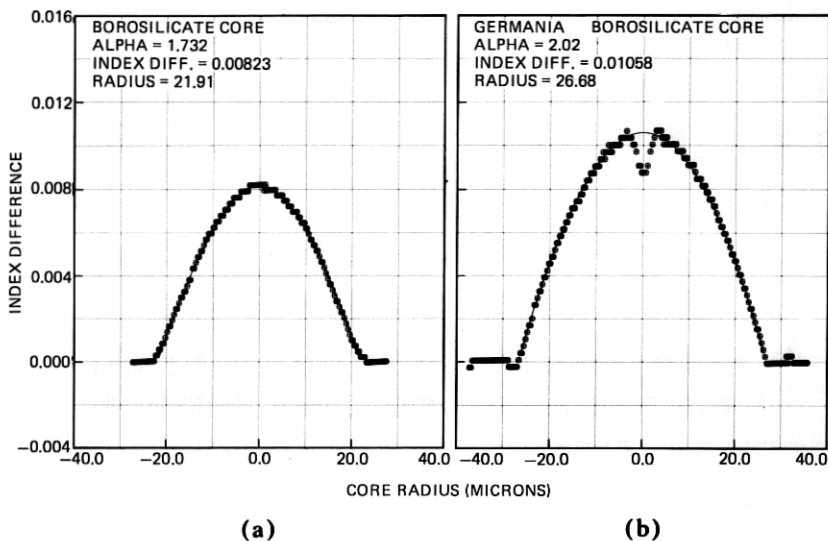


Fig. 1—Refractive-index profiles derived from interference micrographs: (a) a borosilicate graded-core fiber; (b) a germania borosilicate core fiber. The fitted curves are determined from a weighted [eq. (1)] nonlinear least-squares fit to the data \oplus .

II. FIBER FABRICATION AND PROFILE EVALUATION

The borosilicate fibers in this study have a uniform $1 \text{ B}_2\text{O}_3\text{-}6 \text{ SiO}_2$ cladding composition and a core in which the B_2O_3 concentration decreases from 14 mole percent to 0 percent at the center.⁴ Germania borosilicate fibers have a uniform SiO_2 cladding, a thin ($2 \mu\text{m}$) $1 \text{ B}_2\text{O}_3\text{-}9 \text{ SiO}_2$ barrier layer and a core in which the GeO_2 concentration increases from 0 percent to 8.5 mole percent at the center where the material composition is $2 \text{ GeO}_2\text{-}1 \text{ B}_2\text{O}_3\text{-}21 \text{ SiO}_2$. The modified chemical vapor deposition process⁵ is used to deposit the appropriate glass compositions by the reaction of BCl_3 , GeCl_4 , and SiCl_4 with oxygen at a temperature of $1400\text{--}1700^\circ\text{C}$ inside a fused quartz substrate tube. In the case of the borosilicate fibers, the borosilicate cladding is first deposited followed by the graded borosilicate core. The germania borosilicate fibers are typically prepared by depositing 2 borosilicate barrier layers followed by 40–50 graded core layers. The fused quartz support tube is the cladding in this case. The radial index profile is graded by a programmed variation of the chloride dopant concentrations in the reaction stream. After the composite substrate tube is collapsed into a solid preform structure and then drawn into fiber, the resultant index profiles are determined by interference microscopy of thin fiber cross sections.^{6,7}

Figure 1b shows a profile for a typical germania borosilicate fiber. The dip in the center is caused by GeO_2 dopant burn-off during the collapse stage. This type of distortion does not appear in boron graded fibers (Fig.

1a) because the dopant concentration is very small at the core center. The dip at either edge of the germania borosilicate profile corresponds to the borosilicate layer at the core-cladding interface. The index profile parameter, α , is determined by fitting power law profiles to the measured curve. The least-mean-square fit profile is determined from weighted differences between the measured and optimal curves according to:

$$\text{Weighted \% dev.} = \left[\sum_{i=1}^j \frac{(\Delta N_{\text{meas}} - \Delta N_{\text{power law}})^2}{j} W(r_i) \right]^{1/2} \times \frac{100}{\Delta N_{\text{max}}} \quad (1)$$

where

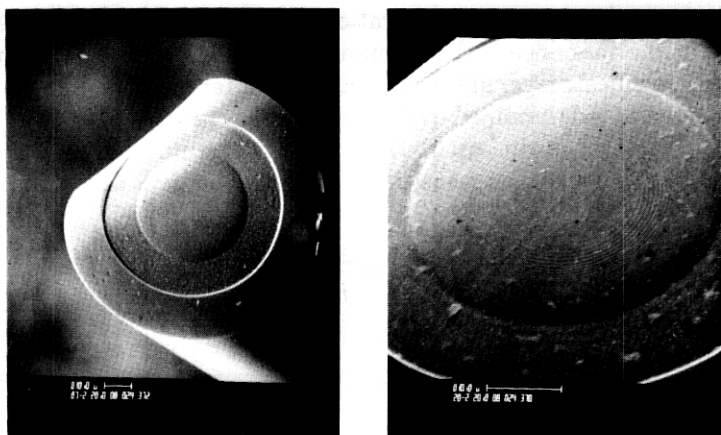
$$W(r_i) = r_i^2 (1 - r_i^2)^{3/2} \quad (2)$$

$$\Delta N_{\text{power law}} = N_{\text{max}} (1 - r_i^\alpha)$$

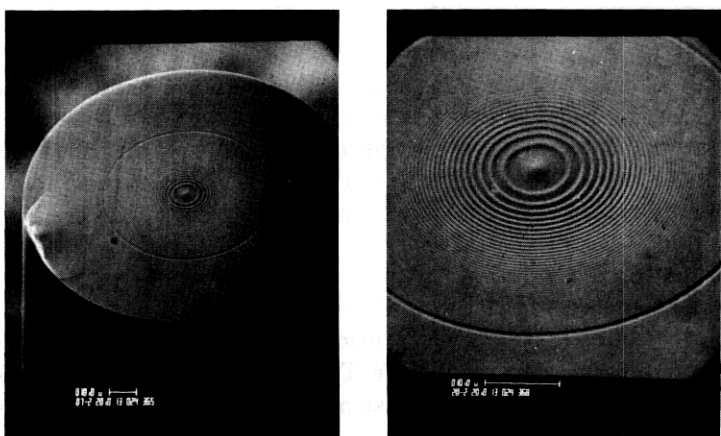
The ΔN 's are index differences and r_i is the distance from the core center divided by the core radius. The weighting function $W(r_1)$ [eq. (2)] was determined⁸ by computing the approximate number of modes that are confined to various sections of the profile. This reduces the importance of the core center, $r_i = 0$, since only the lowest-order modes are confined there and of the profile tail, $r_1 = \pm 1$, which is only important to high-order modes. Maximum weight is placed on the radial region midway between the core and cladding. After obtaining a best fit α , using the weighting function $W(r)$, we determine the unweighted deviations of the data from the calculated profile. Typical unweighted deviations range from 1 to 3 percent from the least-mean-square fit power law profile. However, recent theoretical calculations⁹ have shown that 1 percent profile deviations can cause order-of-magnitude pulsewidth increases from the optimal 2σ (min).

Profile distortions can also be illustrated through scanning electron photomicrographs of etched fiber cross sections as in Fig. 2. The ridged structure midway between core and cladding is in the vicinity of the maximum gradient slope. This ridged distortion is observed in both boron and germania doped fibers, but it appears more prominent in the germania doped fibers due to the high doping in the center where the layers are farther apart. These distortions are due to differences in volatility of the glass components which cause concentration variations in each layer deposited by MCVD.

The concentration of core dopants may be measured directly by the use of electron-beam x-ray microanalysis techniques.¹⁰ An ETEC scanning electron microscope equipped with a KEVEX energy dispersive x-ray spectrometer has been used to measure the germania concentration in



(a) B_2O_3 DOPED FIBERS



(b) GeO_2 DOPED FIBERS

Fig. 2—Scanning electron photomicrographs of etched fiber cross sections illustrate dopant concentration profiles for a boron graded profile and a germania graded profile.

germania borosilicate core fibers as shown in Fig. 3. The high resolution of this technique generates data which more accurately represent the central germania depletion region than the index profile data (Fig. 1b) measured using thin section interference microscopy. The ridged structure seen in the germania borosilicate fiber is coincident with regions of GeO_2 concentration fluctuation. The germania concentration profile characterizes a fiber core in the same way as the refractive index profile, provided the effect of the boron is either independent of radius or negligible. Fitting the weighted power law function to the concentration profile shown in Fig. 3, one obtains an α of 2.12.

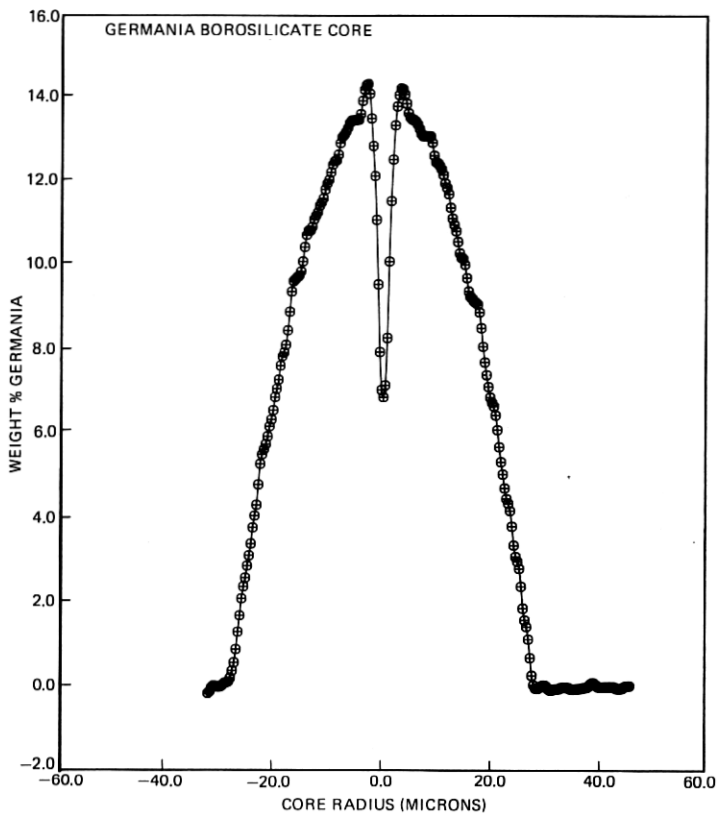


Fig. 3—Germania composition profile for a typical germania borosilicate fiber (the refractive index profile for this same fiber is shown in Fig. 1b).

III. PULSE TRANSMISSION MEASUREMENTS AT $\lambda = 907.5$ nm

Pulse dispersion is characterized at $\lambda = 907.5$ nm by injecting impulses of light (3 dB width = 0.3 nsec, full rms pulsewidth $2\sigma = 0.4$ nsec) from a GaAs laser and measuring the broadened fiber output pulsewidth. The optical shuttle pulse technique^{2,11} is used to make length-dependent pulsewidth measurements by reflecting propagating light back and forth between partially transparent mirrors at the ends of a fiber. Mode-mixing effects were relatively small in all the tested fibers since pulsewidths increased with an almost linear dependence for multi-kilometer path lengths. Therefore, output pulse broadening was primarily caused by intermodal dispersion, profile dispersion, and material dispersion effects due to relative time delays between the source spectral components within its 2.5–3 nm bandwidth.

Material dispersion effects were reduced by a narrowband interference filter which has a 1.4 nm bandwidth approximately centered about the

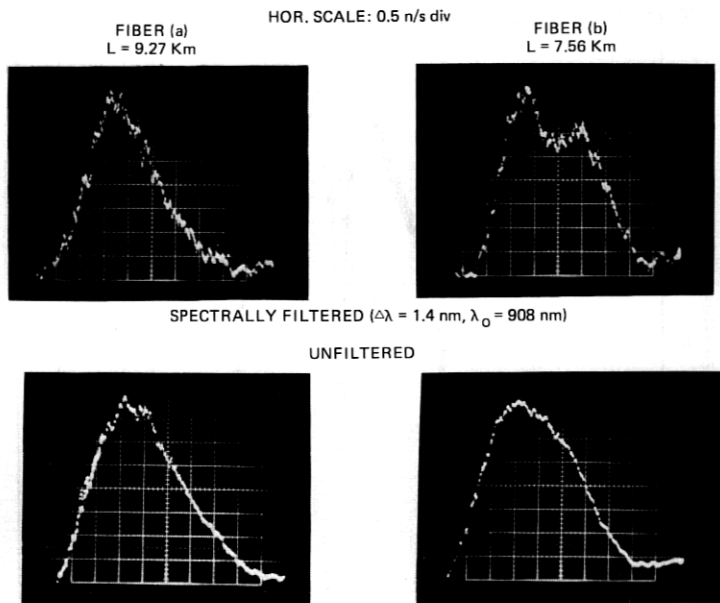


Fig. 4—Material dispersion effects on output pulsewidths from borosilicate fibers (a) and (b). The bottom row of photographs represents pulse propagation of unfiltered GaAs laser light, and the top row represents the propagation of spectrally filtered laser light with bandwidth $\Delta\lambda \approx 1.4$ nm centered about $\lambda_0 \approx 907.5$ nm.

laser line peak at $\lambda = 907.5$ nm. The filtered source spectral bandwidth^{12,13} should cause $2\sigma = 0.09$ nsec/km full rms width pulse spreading in borosilicate fibers and 0.11 nsec/km pulse spreading in germania borosilicate fibers. These kinds of effects are clearly illustrated in Fig. 4 for shuttle pulse extrapolated lengths of 9.27 km for fiber (a) ($L = 1.03$ km) and 7.56 km for fiber (b) ($L = 1.08$ km). The bottom row of photographs shows output pulses due to unfiltered laser light, and the top row of photographs shows pulses due to spectrally filtered light. Results for fiber (a) show that when the source spectral bandwidth is cut in half, the output pulsewidth is reduced by 20 percent. Pulse outputs from fiber (b) show how material dispersion effects mask intermodal effects by smoothing the impulse response. A multipeak pulse structure is recovered by narrowing the laser linewidth.

Far-field spatial filters² (circles and annular rings) are used to measure time-of-flight differences between high- and low-order modes arriving at the fiber output. If high-order modes arrive before low-order modes, the fiber profile is overcompensated because $\alpha < \alpha(\text{opt})$. When high-order modes arrive last, the profile is undercompensated because $\alpha > \alpha(\text{opt})$. Output pulses from fibers with nearly optimal profiles are not altered in shape by spatial ray filters or changed launch conditions. This

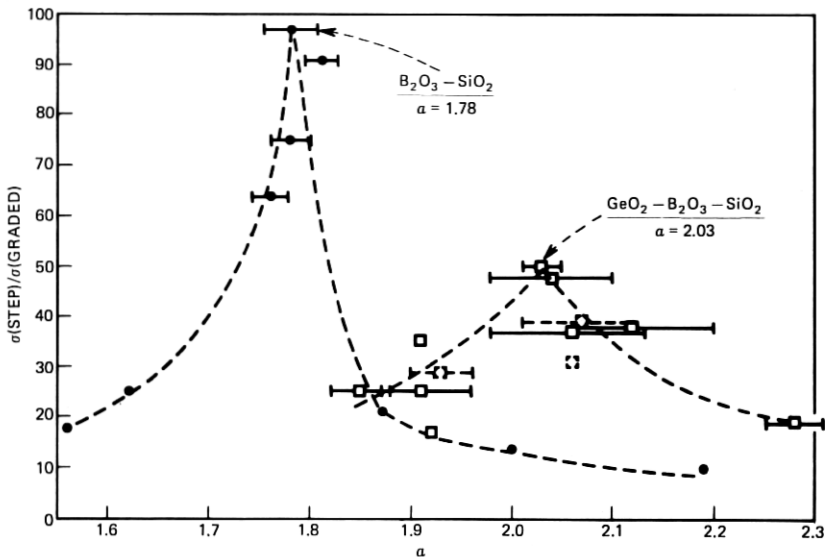


Fig. 5—Root-mean-square pulsewidth reduction factor $\sigma(\text{step})/\sigma(\text{graded}) = [\Delta N L / (12)^{1/2} c] 1/\sigma(\text{graded})$ is plotted vs. α for germania borosilicate and borosilicate fibers. Data points (\square for GBS fibers; \bullet for BS fibers) were obtained by deconvolving expected material dispersion effects (0.12 ns/km for GBS fibers, 0.09 ns/km for BS fibers) from the measured fiber output pulsewidths.

type of profile diagnosis has proved to be a very useful guide for fabricating new fibers with close-to-optimal profile gradients.

Figure 5 summarizes our pulse dispersion data with a plot of the rms pulsewidth reduction factor, $\sigma(\text{step})/\sigma(\text{graded})$, relative to comparable step-index fibers, as a function of α for fibers with different profile gradients. Pulsewidth measurement precision is $2\sigma < 0.07$ ns/km because the optical shuttle pulse technique is used to extrapolate 1 km fiber sample lengths by an order of magnitude. A germania avalanche diode with a response time (2σ) of 0.65 nsec was used as the detector, and all such system broadening was deconvolved from the measured pulsewidths. Data points \bullet were obtained from borosilicate fibers with graded $B_2O_3-SiO_2$ cores and uniform $B_2O_3-SiO_2$ claddings. The three peak data points, which correspond to pulse dispersions of 0.13, 0.14, and 0.15 nsec/km, are results which show that nearly optimal borosilicate fibers can be repeatably fabricated with $2\sigma < 0.2$ ns/km. The optimal profile at $\lambda = 907.5$ nm is characterized by $\alpha(\text{opt}) \approx 1.78$, and the minimum measured pulse dispersion, $2\sigma = 0.13$ ns/km, represents a 100-fold reduction from the theoretical rms pulse spreading in a step-index fiber with $\Delta N \approx 0.0067$ core-to-cladding index difference.

Data points \square were obtained from germania borosilicate fibers with a graded GeO_2 concentration and a nearly uniform B_2O_3 concentration

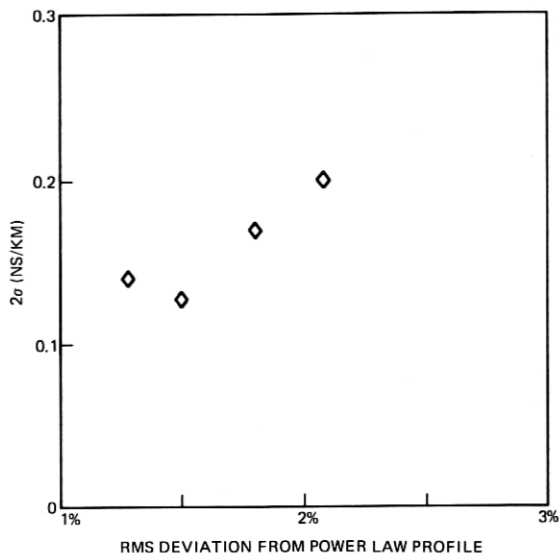


Fig. 6—A plot of the rms deviation, of ΔN vs. r data, from a power law profile vs. pulse dispersion, 2σ , for fibers with near-optimum α values.

across the core. Small amounts of B_2O_3 are added to reduce the viscosity of the core glass, thereby aiding the elimination of bubbles. The two peak \square data points occur when $r/\alpha \approx 2.03$ and correspond to $2\sigma = 0.4$ ns/km and 0.48 ns/km dispersion values. They represent a 50- and 48-fold reduction from the theoretical rms pulse broadening in equivalent step-index fibers with $\Delta N \approx 0.013$. The optimal α values for each type of fiber are consistent with the values predicted by Fleming¹² on the basis of refractive index measurements.

The theoretical minimum pulse broadening in an optimally graded-index fiber is characterized by:¹⁴

$$2\sigma(\min) \approx 141(\Delta N)^2 \quad (3)$$

The theoretical maximum pulsewidth reduction factor is given by:

$$\left(\frac{\sigma(\text{step})}{\sigma(\text{graded})} \right)_{\max} = \frac{1}{\sqrt{12}} \frac{\Delta NL/c}{\sigma(\min)L} = \frac{14}{\Delta N} \quad (4)$$

which is inversely proportional to ΔN , the maximum core-to-cladding index difference. Therefore, the ratio of 2 between the peak pulsewidth reduction factors for the borosilicate and germania borosilicate fibers in Fig. 5 is consistent with the fact that $\Delta N(\text{GBS}) \sim 2\Delta N(\text{BS})$. However, the measured pulsewidths are 18 to 30 times greater than the minimum values predicted by eq. (3) [$2\sigma(\min) \sim 0.007$ ns/km for borosilicate fibers with $\Delta N \approx 0.007$; $2\sigma(\min) \sim 0.024$ ns/km for germania borosilicate fibers with $\Delta N \sim 0.013$].

Two possible reasons for the measured dispersion being so much larger than the theoretical minimum value are (i) the profile α value varies along the length of the fiber, or (ii) the profile is not exactly a power law shape. Each of these differences probably applies to some degree. We have attempted to correlate the rms deviations from a power law profile with the pulse dispersion for fibers which have nearly optimal α values.⁹ The influence of the refractive index dip in the germania-doped fiber profile was too large for us to obtain any meaningful comparison. In the case of the borosilicate fibers, which have a smoother profile, a rough correlation can be found. Figure 6 demonstrates this possible correlation for fibers with $\alpha = 1.8 \pm 0.05$. These data are far from conclusive, but it is clear that further significant pulsewidth reduction will require improved control of the refractive index profile so that it conforms to the correct power law function more exactly than the present fibers. Development of these improvements will require substantial improvements in MCVD deposition control and in fiber profile measurement.

IV. CONCLUSIONS

Pulse transmission properties have been compared for two of the most common types of high silica graded-index fibers. A spectral filter was used to reduce material dispersion effects caused by a GaAs injection laser at $\lambda = 907.5$ nm and the optical shuttle pulse technique was used to make precise intermodal pulse dispersion measurements.

Nearly optimal profile gradients are characterized by $\alpha \approx 2.03$ in germania borosilicate fibers and by $\alpha \approx 1.78$ in borosilicate fibers. Resultant pulsewidth reduction factors are approximately 50 for germania graded fibers with $\Delta N \approx 0.013$ (N.A. ≈ 0.19) and 100 for boron graded fibers with $\Delta N \approx 0.0067$ (N.A. ≈ 0.14). The factor-of-2 ratio between the peak pulsewidth reduction factors for the two kinds of fiber is consistent with the fact that $\Delta N(\text{GBS}) \approx 2\Delta N(\text{BS})$. However, the measured pulsewidths are 18 to 30 times greater than the minimum values predicted by $2\sigma(\text{min}) \sim 300\Delta^2$ ns/km. Further significant pulsewidth reductions will require improved profile control to reduce by an order of magnitude current 1–3 percent rms deviations between fabricated profiles and optimum power law shapes.

The results in this paper apply at a design wavelength, $\lambda = 907.5$ nm, corresponding to a GaAs injection laser. A companion paper³ describes how profile dispersion affects fiber transmission bandwidths at other wavelengths.

REFERENCES

1. L. G. Cohen, G. W. Tasker, W. G. French, and J. R. Simpson, "Pulse Dispersion in Multimode Fibers with Graded B_2O_3 - SiO_2 Cores and Uniform B_2O_3 - SiO_2 Cladding," *Appl. Phys. Lett.*, 28 (April 1976), pp. 391–393.
2. L. G. Cohen, "Pulse Transmission Measurements for Determining Near Optimal

- Profile Gradings in Multimode Borosilicate Optical Fibers," *Appl. Opt.*, *15* (July 1976), pp. 1808-1814.
3. L. G. Cohen, I. P. Kaminow, H. W. Astle, and L. W. Stulz, "Profile Dispersion Effects on Transmission Bandwidths in Graded Index Optical Fibers," *IEEE J. Quant. Electron.*, *14* (January 1978), pp. 37-41.
 4. W. G. French, G. W. Tasker, and J. R. Simpson, "Graded Index Fiber Waveguides with Borosilicate Composition: Fabrication Techniques," *Appl. Opt.*, *15* (July 1976), pp. 1803-1807.
 5. J. B. MacChesney, P. B. O'Connor, F. V. DiMarcello, J. R. Simpson, and P. D. Lazay, "Preparation of Low Loss Optical Fibers Using Simultaneous Vapor Deposition and Fusion," *Proc. 4th Int. Cong. on Glass, Kyoto, Japan, 6-40* (July 1974).
 6. H. M. Presby, W. Mammel, and R. M. Derosier, "Refractive Index Profiling of Graded Index Optical Fibers," *Rev. Sci. Instrum.*, *47* (March 1976), pp. 348-352.
 7. B. C. Wonsiewicz, W. G. French, P. D. Lazay, and J. R. Simpson, "Automatic Analysis of Interferograms: Optical Waveguide Refractive Index Profiles," *Appl. Opt.*, *15* (April 1976), pp. 1048-1052.
 8. D. Gloge, private communication.
 9. E. A. J. Marcatili, "Modal Dispersion in Optical Fibers with Arbitrary Numerical Aperture and Profile Dispersion," *B.S.T.J.*, *56*, No. 1 (January 1977), pp. 49-63.
 10. J. W. Fleming and Luis Soto, "SEM Microanalysis of Germanium Borosilicate Optical Waveguides," *Proc. of Pittsburgh Conf. on Analytical Chemistry and Applied Spectroscopy, Paper No. 197, February 1977*.
 11. L. G. Cohen, "Shuttle Pulse Measurements of Pulse Spreading in an Optical Fiber," *Appl. Opt.*, *14* (June 1975), pp. 1351-1356.
 12. J. W. Fleming, "Measurements of Dispersion in $\text{GeO}_2\text{-B}_2\text{O}_3\text{-SiO}_2$ Glasses," *J. Amer. Cer. Soc.*, *59* (November-December 1976), pp. 503-507.
 13. L. G. Cohen and C. Lin, "Transmission Measurements of Zero Material Dispersion in Optical Fibers," *CLEA Conf., Washington, D.C., Paper PD 5.12, June 1977*, abstract in *IEEE J. Quant. Electron.*, *13* (September 1977), pp. 91D-92D; "Pulse Delay Measurements in the Zero Material Dispersion Wavelength Region for Optical Fibers," *Appl. Opt.*, *16* (December 1977), pp. 3136-3139.
 14. J. A. Arnaud and J. W. Fleming, "Pulse Broadening in Multimode Optical Fibers with Large $\Delta n/n$. Numerical Results," *Electron. Lett.*, *12* (April 1976), pp. 167-169.